ORGANOMETALLICS

Article

pubs.acs.org/Organometallics

The Negishi Catalysis: Full Study of the Complications in the Transmetalation Step and Consequences for the Coupling Products

Juan del Pozo,[†] Gorka Salas,[‡] Rosana Álvarez,[*,§] Juan A. Casares,[*,†] and Pablo Espinet[*,†]

[†]IU CINQUIMA/Química Inorgánica, Facultad de Ciencias, Universidad de Valladolid, 47011 Valladolid, Spain

[‡]IMDEA Nanociencia, Ciudad Universitaria de Cantoblanco, 28049 Madrid, Spain

[§]Departamento de Química Orgánica, Facultad de Química (CINBIO), Universidade de Vigo, Campus As Lagoas-Marcosende, 36310 Vigo, Spain

Supporting Information

ABSTRACT: In addition to the expected products, *trans*- and *cis*-[PdRfMe(PPh_3)$_2$], the transmetalation between $ZnMe_2$ and *trans*-[PdRfCl(PPh_3)$_2$] yields [PdMeCl(PPh_3)$_2$] and ZnRfMe as the result of secondary transmetalation processes. ZnRfMe is also formed by reaction of *trans*- and *cis*-[PdRfMe(PPh_3)$_2$] with $ZnMe_2$. The different competitive reaction mechanisms that participate in the transmetalations have been studied by experiments and by DFT calculations. The relative contribution of each reaction pathway in the formation of the unwanted product ZnRfMe has been measured. The effect of excess ligand (PPh_3) on the several transmetalations has been established.

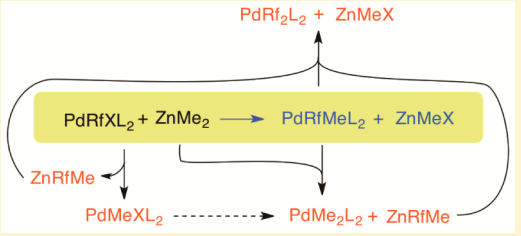

INTRODUCTION

The Negishi reaction is a powerful process for the formation of C−C bonds.[1,2] In fact, it is the reaction of choice for couplings involving sp^3 carbons, due to the high reactivity of organozinc reagents.[3−5] The coupling of alkyl groups from organoboron and organotin organometallics is usually very sluggish unless highly nucleophilic activators are used to facilitate the transmetalation step. In sharp contrast, organozincs have been shown to transmetalate to Pd at temperatures as low as −60 °C,[6] which allows for remarkably facile coupling of alkyl groups, even secondary alkyls.[7] For other palladium-catalyzed couplings of organic electrophiles (R^1X) and nucleophiles (MR^2), the reaction pursues the selective formation of R^1−R^2, but frequently homocoupling byproducts, presumably formed via undesired transmetalations, contaminate the result.[8] In 1994 van Asselt and Elsevier showed that these homocoupling products could arise from undesired reactions that exchange the organic group in the nucleophile by another organic group at the palladium, rather than by the halogen (Scheme 1a). Thus, in the reaction of [PdBzBr(ArBIAN)] (Bz = benzyl; Ar-BIAN = bis(arylimino)acenaphthene) with ZnTolCl they found that the exchange produced the observable Bz/Tol intermediate [PdTolBr(ArBIAN)], which after subsequent Br/Tol transmetalation led to $(MeC_6H_4)_2$ as the main reaction product.[9]

A second report, this time involving C(sp^3) in the coupling, came some years later from our group, when we found that the transmetalation of *trans*-[PdRfCl(PPh_3)$_2$] (**1**; Rf = 3,5-dichloro-2,4,6-trifluorophenyl) with $ZnMe_2$ or with ZnMeCl produced, in addition to the two expected palladium complexes *trans*-[PdRfMe(PPh_3)$_2$] (**2**) and *cis*-[PdRfMe(PPh_3)$_2$] (**3**), large amounts of ZnRfMe, ZnRfCl, and [$PdMe_2$(PPh_3)$_2$].[10] Following our observation Lei et al. reported the formation of

Scheme 1. Previous Results

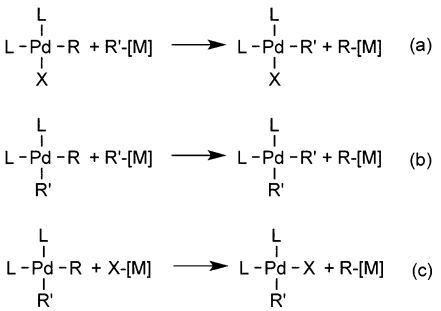

undesired aryl exchanges between zinc and palladium (Scheme 1b), as well as the formation of homocoupling biaryls, in the Pd-catalyzed coupling of Ar^1I with $ZnAr^2Cl$.[11a] They suggested that the Ar^1−Ar^2 to Ar^2−Ar^2 ratio found in the products was the result of a kinetic competition between reductive elimination and aryl exchange reaction rates on a [$PdAr^1Ar^2$(dppf)] intermediate.

In Negishi syntheses, where halides are always present (introduced in the initial oxidative addition step of ArX to Pd^0), the study of the undesired reactions shown in Scheme 1a,b is obscured by the interference of retrotransmetalation reactions (Scheme 1c).[12] A good starting point to analyze these complicated systems is to dissect the study by starting with the reactivity of complexes [PdArAr′L_2] with ZnR_2 derivatives, which provides a particular scenario where halides (hence the reactions in Scheme 1a,b) are absent. These complexes are

Received: August 16, 2016
Published: September 30, 2016

DOI: 10.1021/acs.organomet.6b00660
Organometallics 2016, 35, 3604−3611

well-known intermediates in cross-coupling reactions. The reductive elimination of two sp^2 carbons from *cis*-[PdArAr′L_2] is usually fast,[13] but in instances that disfavor reductive elimination (e.g., electron-withdrawing groups in the carbon fragments or large steric hindrance), the undesired transmetalations shown in Scheme 1 can become a serious competition to the expected Ar−Ar′ cross-coupling.[14] Furthermore, the reductive elimination step in coupling reactions involving sp^3 carbon atoms is usually slow,[13] and in the search for Ar−alkyl coupling reactions these undesired transmetalations may become an efficient path to undesired Ar−Ar products.[8] Moreover, we have recently shown that there are cis/trans isomerization reactions of [PdRR′L_2] complexes (R = Me; R′ = Me, 3,5-dichloro-2,4,6-trifluorophenyl (Rf)) that are mechanistically associated with transmetalations because they share a common intermediate. This further complicates the reaction scheme during the cross-coupling reaction.[15] From a positive point of view, all of these model systems with high coupling barriers to the desired product create a landscape where the undesired side processes can be more easily studied.

Herein we report kinetic experiments and DFT computational studies to understand the complications disturbing the desired ideal Negishi process, by examining the reactivity of [PdMeArL$_2$] (cis and trans, Ar = C_6F_5, $C_6F_3Cl_2$) complexes with $ZnMe_2$ and other secondary transmetalations. The computational studies provide features of the structures participating in the transmetalations, stereochemistry at palladium, additional intermediates or transition states that cannot be kinetically deduced, structural details of the exchange process, etc.[16] The graphical presentation of the process is made in a unified manner; thus, the reaction profiles will contain experimental and calculated values for comparison but, obviously, not every calculated structure has a measured experimental energy. For instance, energies of species after the rate-determining state cannot be experimentally measured.[17]

RESULTS AND DISCUSSION

In the Negishi process (also in others) we can define two categories of transmetalation, depending on the groups undergoing exchange: (i) primary transmetalations, in which an R group on Zn is exchanged for an X group (usually a halide) on Pd (*X for carbon exchange*), and (ii) secondary transmetalations, meaning transmetalations that exchange two R fragments between Pd and Zn (*carbon for carbon exchanges*). Other possible combinations as transmetalations where an X group on Zn were exchanged for an R group on Pd are usually thermodinamically unfavorable.

The first step in the PdL$_n$-catalyzed (L = PPh_3) Negishi coupling of RfX (X^- = halide) with $ZnMe_2$ is the oxidative addition of RfX to PdL$_n$, producing [PdRfXL$_2$] (**1**; Rf = $C_6F_3Cl_2$).[18] Then, in the transmetalation step, only the exchanges involving nonidentical groups are synthetically relevant and observable by NMR, in addition to the isomerization of the Pd complexes. With these conditions, the most relevant exchanges of different groups (taken in both senses of the equilibrium) are shown in Chart 1.[19]

The only desired transmetalation (X for Me) is the primary transmetalation in eq 1 of Chart 1, leading to [PdRfMeL$_2$], which is the complex precursor of the cross-coupling product. However, an undesired secondary transmetalation (Rf for Me) can take place with the same reagents (eq 2), leading to [PdMeXL$_2$]. Another possible undesired secondary transmetalation (eq 3) consumes [PdRfMeL$_2$] to produce undesired

Chart 1. Primary and secondary transmetalations (cis/trans isomers not specified for simplicity)

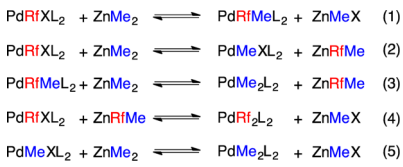

PdMe$_2$L$_2$, a potential source of Me−Me homocoupling. Equations 2 and 3 produce previously nonexistent Pd complexes or Zn reagents that are a potential source of new primary transmetalations, now undesired, as shown in eq 4 (forming a potential source of Rf−Rf homocoupling), and eq 5 (along with eq 3, forming a potential source of Me−Me homocoupling).

To organize the discussion we consider the exchanges in the following three sections.

Analysis of the Primary Cl/Me Transmetalation Exchange on *trans*-[PdRfCl(PPh$_3$)$_2$] (1) with ZnMe$_2$, Complicated by Secondary Rf/Me Transmetalations. Some time ago we reported that the transmetalation reaction between *trans*-[PdRfCl(PPh$_3$)$_2$] (**1**) and $ZnMe_2$, run at 25 °C in THF with a 20:1 excess of $ZnMe_2$, produces not only *trans*- and *cis*-[PdRfMe(PPh$_3$)$_2$] (**2** and **3**, respectively) and ZnMeCl but also a large amount of the exchange products ZnRfMe and [PdMe$_2$(PPh$_3$)$_2$] (Scheme 2).[10]

Scheme 2. Our Previous Results[10]

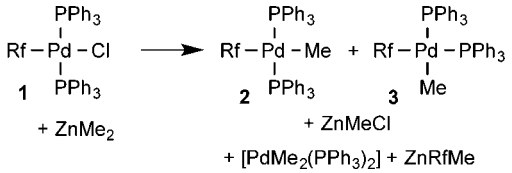

We have studied here the effect of an excess of ligand in that system. Figure 1 plots the disappearance of **1**, and the formation of the different products, in the reaction of *trans*-[PdRfCl(PPh$_3$)$_2$] (**1**) with a fixed excess of $ZnMe_2$ (Zn:Pd = 10:1), in solutions with increasing amounts of PPh_3.

The data in Figure 1 show that the rate of consumption of **1** depends on $[PPh_3]^-$, meaning that, as in many other transmetalation processes with other nucleophiles, the first step in the transmetalation involves the substitution of PPh_3 by the incoming $ZnMe_2$. The same holds for the initial formation of *trans*-[PdRfMe(PPh$_3$)$_2$] (**2**), which is the main product at short reaction times, and ZnClMe (not detectable in the ^{19}F spectrum).

Regarding the formation of *cis*-[PdRfMe(PPh$_3$)$_2$] (**3**) and ZnRfMe, the interpretation of the data is less clear-cut: their experimental kinetic orders are 0.2 and 0.3, respectively,[20] suggesting that these species are involved in several reactions that have different dependences on the concentration of PPh_3. We have shown in a previous study that the isomerization of **3** to **2** is phosphine dependent and can be catalyzed by $ZnMe_2$.[15] For ZnRfMe the situation is even more complex, since ZnRfMe is formed in two ways: (i) through the secondary transmetalations between **2** or **3** and $ZnMe_2$ and (ii) by direct Me/Rf exchange between **1** and $ZnMe_2$. The dependence of these processes on the concentration of PPh_3 has not been established so far. There are other possible sources of ZnRfMe,

DOI: 10.1021/acs.organomet.6b00660
Organometallics 2016, 35, 3604−3611

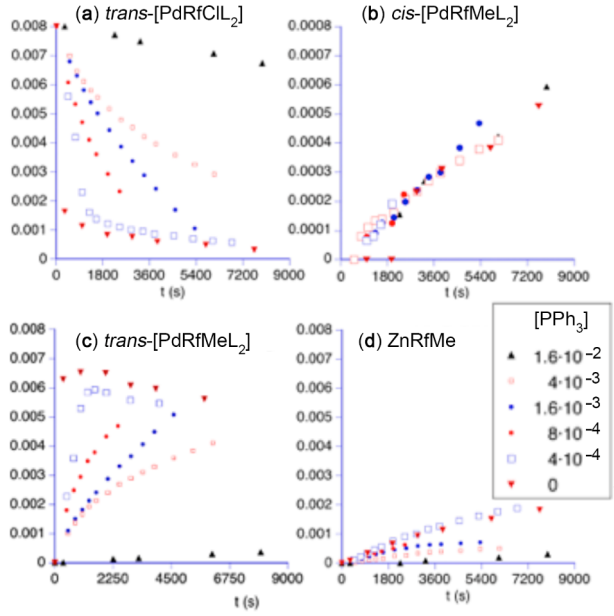

Figure 1. Experimental concentration versus time plots for the transmetalation reaction of *trans*-[PdRfCl(PPh_3)$_2$] with $ZnMe_2$ under different concentrations of PPh_3: (a) *trans*-[PdRfCl(PPh_3)$_2$] (**1**); (b) *cis*-[PdRfMe(PPh_3)$_2$] (**3**); (c) *trans*-[PdRfMe(PPh_3)$_2$] (**2**); (d) ZnRfMe. Note the different scale for the concentrations of *cis*-[PdRfMeL$_2$] (Figure 1b). The data have been obtained by integration of ^{19}F NMR spectra.

such the retrotransmetalation of ZnMeCl with **2** or **3**, but these are not significant under the very low concentration of ZnMeCl existing at the beginning of the reaction; consequently, retrotransmetalation pathways cannot explain the high rate of formation of ZnRfMe observed at short reaction times.

Although the bizarre kinetic order for the formation of *cis*-[PdRfMe(PPh_3)$_2$] (**3**) and ZnRfMe suggests the competition of several mechanisms, it is not possible to quantify the reaction parameters unless the reactions of **2** and **3** with $ZnMe_2$ are addressed first.

Analysis of the Secondary Rf/Me Transmetalation Exchanges on *trans*- and *cis*-[PdRfMe(PPh_3)$_2$] with $ZnMe_2$. The reactions of *trans*- and *cis*-[PdMeRf(PPh_3)$_2$] (**2** and **3**, respectively) with $ZnMe_2$ in THF were studied at 298 K by monitoring the Rf/Me exchange with ^{19}F and ^{31}P NMR. When a large excess of $ZnMe_2$ was employed (as this is a condition of Negishi cross-coupling reactions), the transmetalation equilibrium was shifted toward the formation of ZnRfMe. Under these conditions the isomerization of *trans*- to *cis*-[$PdMe_2(PPh_3)_2$] is very fast; thus, eventually both isomers, *cis*- and *trans*-[PdRfMe(PPh_3)$_2$], are transformed into *cis*-[$PdMe_2(PPh_3)_2$], which is the thermodynamically highly favored isomer (Scheme 3).

The reaction rates were measured in experiments with added PPh_3.[21] Under these conditions the kinetic influence of reductive elimination of Rf–Me or Rf–Rf is negligible. The reaction orders on the concentration of PPh_3 were obtained for **2** and **3** from the initial rates, and kinetic rate constants were obtained by nonlinear least-squares fitting of the data. The experimental $\Delta G^{\ddagger}$ values are represented, along with the calculated values, in the reaction profile in Figure 2.

The experimental studies for the *cis* isomer **3** show that the free ligand retards the formation of ZnRfMe. The process has a rough order of −1 (slope −0.9 based on initial rates of

Scheme 3. Formation of *cis*-[$PdMe_2L_2$] by Secondary Transmetalations Involving Complexes 2 and 3

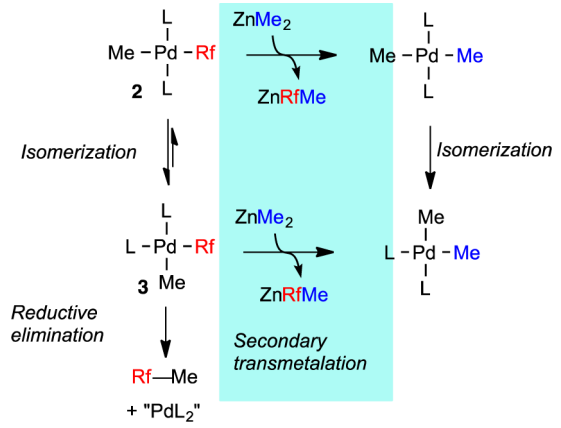

formation of ZnRMe; see the Supporting Information) with respect to the concentration of PPh_3, and the plot of r_0^{-1} versus the concentration of PPh_3 added is a straight line. This is consistent with a mechanism in which the first step is the substitution of one phosphine ligand by $ZnMe_2$, producing the intermediate [PdRfMeL–$ZnMe_2$], prior to the transmetalation step (eqs 6–8 in Chart 2). When the experimental values were fitted to this model, the activation energies for the phosphine dissociation (22.4 kcal/mol) and for the Rf/Me exchange (25.7 kcal/mol) were obtained for complex **3**.

The proposed pathways were studied by DFT methods (wB97XD/PCM(THF)/6-31G*-SDD//B3LYP/6-31G*-SDD), and the results are shown in Figure 2.[22−24] The overall mechanism resembles a double-substitution process and is similar to that found for the $ZnMe_2$-catalyzed isomerization of **3** to **2**.[15]

Starting with *cis*-[PdArMe(L)$_2$] (**3**) and following the ligand substitution pathway in Figure 2, the calculations propose first a very weak interaction with $ZnMe_2$, which was commented on in a previous paper and has no kinetic significance.[15] In the transition state ***TSI1*** the Zn–Me[2] bond acts as an incoming ligand, releasing one PPh_3 (L[2]) from the palladium, while the zinc takes electron density from the Rf–Pd bond, affording intermediate $\mathbf{I_1}$, with the exchanging Me involved in a 3c-2e bond. The second substitution takes place so that the incoming ligand is PPh_3 and the leaving ligand is the Rf–Zn bond (***TSI2***). The activation energies for these transition states (19.5 and 22.7 kcal/mol, respectively) fit very well with the experimental values obtained (22.4 and 25.7 kcal/mol, respectively). Note that this pathway produces cis to trans isomerization of the PPh_3 ligands, yielding *trans*-[$PdMe_2L_2$], but the $ZnMe_2$-catalyzed isomerization to *cis*-[$PdMe_2L_2$] is fast.

The putative reaction without ligand substitution for *cis*-[PdArMe(L)$_2$] was also studied by DFT (Figure 2, ligand-independent mechanism) and consists of a rather common associative interchange of Me and Rf via a double bridge (with Pd–Zn bond participation). The PPh_3 ligands remain cis throughout the process. The participation of this pathway appears to be unimportant, since it shows a much higher activation energy (30.3 kcal/mol).

The reaction of *trans*-[PdRfMe(PPh_3)$_2$] with $ZnMe_2$ was studied under the same experimental conditions. In this case the dependence of the reaction rate on the concentration of PPh_3 was very small (the experimental order of the secondary transmetalation reaction is −0.3). This suggests the partic-

DOI: 10.1021/acs.organomet.6b00660
Organometallics 2016, 35, 3604−3611

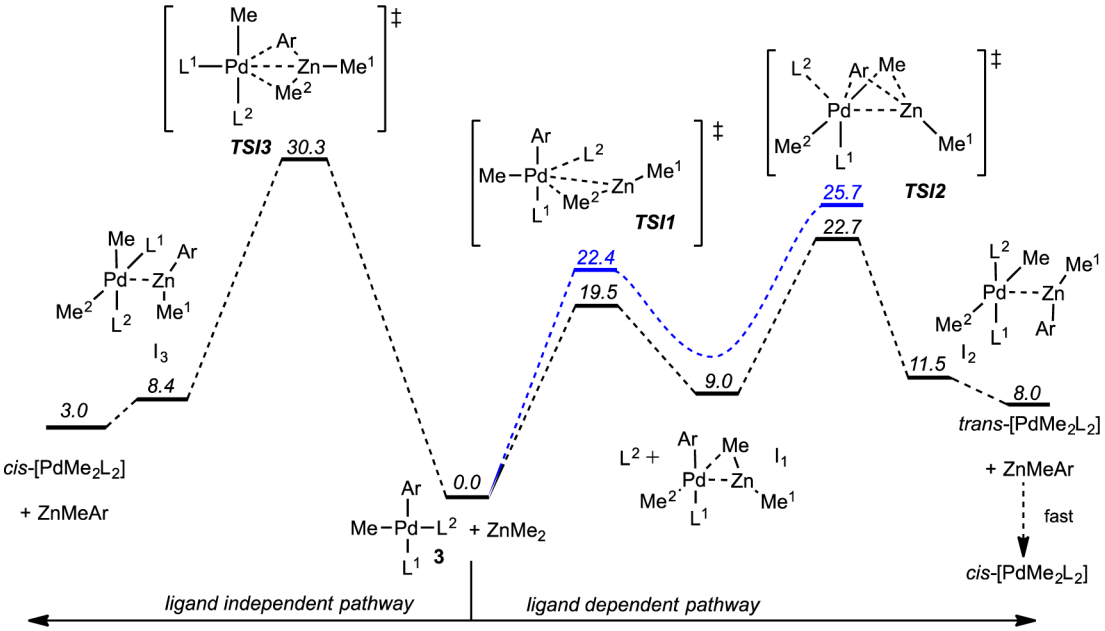

Figure 2. DFT profiles (in black; wB97XD/PCM(THF)/6-31G*-SDD//B3LYP/6-31G*-SDD; Ar = Pf and $L_1 = L_2 = PPh_3$) and experimental energy values (in blue; Ar = Rf) for the mechanisms proposed for the secondary transmetalation (ligand-dependent and -independent pathways) in the reaction between *cis*-[PdArMe(L)$_2$] (**3**) and $ZnMe_2$ ($\Delta G^{\ddagger}$ values are given in kcal/mol). Obviously the calculated energy for the intermediate connecting ***TSI1*** and ***TSI2*** makes its formation slower than its disappearance; thus, it cannot be observed experimentally.

Chart 2. Proposed Mechanism for Me/Rf Exchange between Zn and Pd in the Reaction of *cis*-[PdRfMe(PPh$_3$)$_2$] (3) with $ZnMe_2$

cis-[PdRfMeL$_2$] + $ZnMe_2$ ⇌ *cis*-[PdRfMeL(ZnMe$_2$)] + L (6)

cis-[PdRfMeL(ZnMe$_2$)] → [PdMeMeL(ZnRfMe)] (7)

[PdMeMeL(ZnRfMe)] + L ⇌ (fast) [PdMeMeL$_2$] + ZnRfMe (8)

ipation of two competitive pathways: one independent of the phosphine concentration and another (slower but not negligible) dependent (Scheme 4). The experimental data fit well to this kinetic model, although the system contains too many variables to be fully resolved.[25,26]

Scheme 4. Rf/Me Secondary Transmetalation on *trans*-[PdRfMe(PPh$_3$)$_2$]

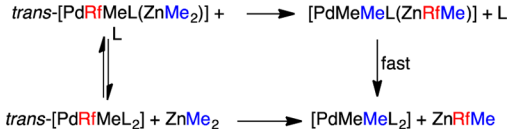

Figure 3 shows the DFT profiles starting with *trans*-[PdArMe(L)$_2$] (**2**) and $ZnMe_2$ for both mechanisms (ligand-substitution and ligand-independent mechanisms). The ligand substitution pathway that takes place in a single step (ligand independent) is again an associative exchange of Me and Rf via the doubly bridged transition state ***TSI6***. The calculated activation energy is $\Delta G^{\ddagger}$ = 26.4 kcal/mol (experimental, 23.7 kcal/mol). As for the cis complex, there is no PPh_3 isomerization in this pathway.

The higher efficiency of the direct Rf/Me exchange in the trans complex **2**, confirming activation energy lower than that for the cis complex **3**, is due to the large trans influence of the Me group, which induces electron density into the Ar group, making the bridge where it participates in ***TSI6*** less electron deficient, consequently stabilizing this transition state. Although the product of transmetalation through this pathway is *trans*-[PdMe$_2$L$_2$], under the reaction conditions it isomerizes quickly to *cis*-[PdMe$_2$L$_2$], as already discussed.

The phosphine-dependent pathway starting from the trans isomer (Figure 3) is a double-substitution process similar to that discussed above for the reaction of the cis isomer and for the previously reported isomerization catalyzed by $ZnMe_2$ of **2** to **3**.[15] This pathway directly yields *cis*-[PdMe$_2$L$_2$]. The activation energy is very similar to that of the phosphine-independent pathway, and this explains the −0.3 dependence order on PPh_3 concentration.

The studies in this section show that both isomers, **2** and **3**, are able to suffer secondary transmetalations under the conditions in which the main reaction (primary transmetalation on **1**) takes place, eventually producing *cis*-[PdMe$_2$L$_2$]. With PPh_3 as ligand, the ligand-independent pathway prevails for **3** and is in competition with the ligand-dependent pathways for **2**. Due to these ligand-independent pathways, the addition of excess ligand cannot completely inhibit the secondary transmetalations. It seems that one plausible solution to suppress them might be the use of ligands that make stronger Pd−L bonds: this would inhibit their substitution by alkylzinc reagents, quenching the ligand-dependent pathway. Calculations for the stronger ligand PMe_3 for comparison (Table 1) show a more complex behavior.[24] For complex **3** and the ligand-dependent pathway (Figure 2) the rate-determining $\Delta G^{\ddagger}$ value certainly increases from 22.7 to 23.9 kcal mol^{-1}, but this difference involves a change of transition state from ***TSI2*** to ***TSI1***. In fact, the large effect upon ligand change occurs in ***TSI1***, which changes from 19.5 to 23.9 kcal mol^{-1}. In addition, a significant change is produced in the competitive ligand-independent pathway, for which ***TSI3*** changes from 30.3 to 25.7 kcal mol^{-1}, increasing its global contribution to the reaction. However, for complex **2** and the ligand-dependent

DOI: 10.1021/acs.organomet.6b00660
Organometallics 2016, 35, 3604−3611

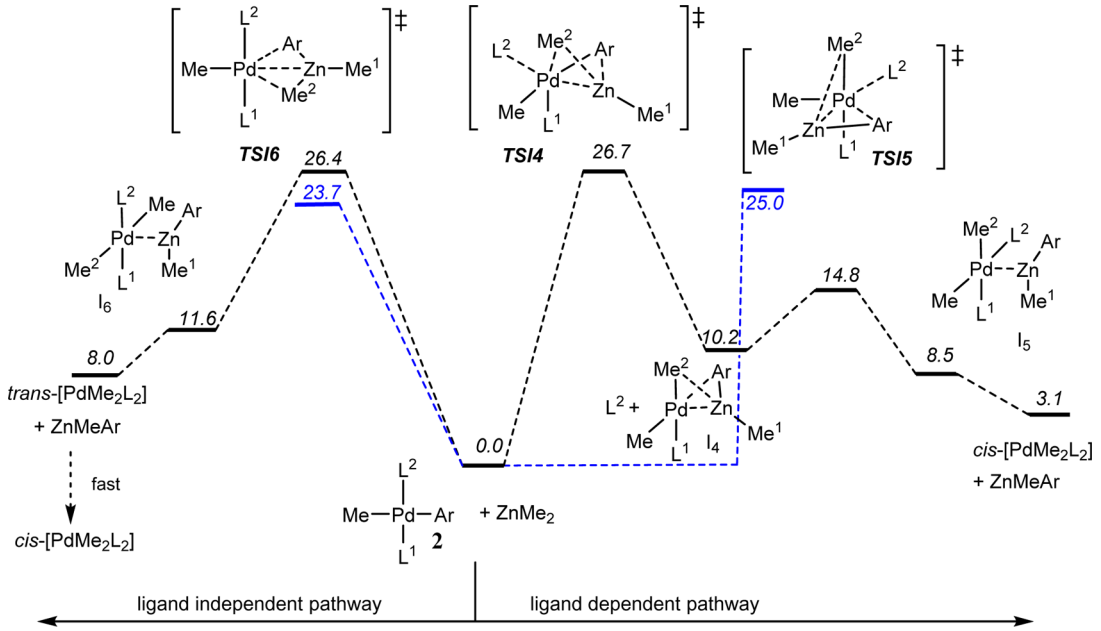

Figure 3. DFT profiles (shown in black; wB97XD/PCM(THF)/6-31G*-SDD//B3LYP/6-31G*-SDD; Ar = Pf and $L_1 = L_2 = PPh_3$) and experimental energetic values (shown in blue; Ar = Rf) for the mechanisms proposed for the secondary transmetalation (ligand-dependent and -independent pathways) in the reaction between *trans*-[PdArMe(L)$_2$] (**2**) and $ZnMe_2$ ($\Delta G^{\ddagger}$ values are given in kcal/mol).

Table 1. $\Delta G^{\ddagger}$ (kcal/mol) for the Transition States of the Pathways in the Reaction between *trans*- or *cis*-[PdArMe(L)$_2$] (2, 3) and $ZnMe_2$ (L = PMe_3, PPh_3)

	3			2		
	***TSI*$_1$**	***TSI*$_2$**	***TSI*$_3$**	***TSI*$_4$**	***TSI*$_5$**	***TSI*$_6$**
PMe_3	23.9	21.4	25.7	24.3	23.4	22.7
PPh_3	19.5	22.7	30.3	26.7	14.8	26.4

pathway transition (Figure 3) a small decrease in $\Delta G^{\ddagger}$ from 26.7 to 24.3 kcal mol^{-1}, this time associated with only one transition state (***TSI4***), is observed, whereas the large increase (from 14.8 to 23.4 kcal mol^{-1}) occurs in ***TSI5*** and is insufficient to produce an overall increase for this pathway. For this isomer the stabilization of ***TSI6*** (from 26.4 to 22.7 kcal mol^{-1}) in the ligand-independent pathway is favored for L = PMe_3, frustrating the otherwise beneficial effect of using a strong donor ligand. Thus, how much the transition states are affected is not easy to guess when the cis and the trans isomers are compared.

Somehow against our initial expectations, the transition states of the simpler ligand-independent pathway are highly stabilized for the better donor ligand PMe_3 for both isomers (***TSI3*** and ***TSI6***) and the secondary transmetalations become more competitive, totally frustrating this solution to the problem. In fact, the transition state of the pathways that we have been calling "ligand independent" because a ligand is not released are ligand dependent through the electronic effect of the ancillary ligand on the bridges, which are less electron deficient for stronger donor ancillary ligands.

From a practical point of view the conclusion of this section is that the best way to address this problem and reduce the incidence of these undesired secondary transmetalations seems to be the use of ligands that accelerate the reductive elimination.

Analysis of the Secondary Rf/Me Transmetalation Exchange on *trans*-[PdRfCl(PPh_3)$_2$] (1) with $ZnMe_2$. Now, having determined independently the rates for the isomerization between **2** and **3** and for the secondary Rf/Me transmetalations in the reaction between *cis*- or *trans*-[PdArMe(PPh_3)$_2$] and $ZnMe_2$, it is possible to revisit our initial study on *trans*-[PdRfCl(PPh_3)$_2$]. Figure 4 shows the course of the transmetalation experiment of *trans*-[PdRfCl(PPh_3)$_2$] (**1**) and $ZnMe_2$. In order to fit the observed results, we carry out an overall kinetic simulation including the primary Cl/Me substitution and all of the previous observations (Scheme 5), taking into account the isomerization and the two profiles (ligand-dependent and ligand-independent mechanisms) discussed in the previous section. In these simulations the rate constants of the secondary transmetalations on **2** and **3**, the **2**/**3** isomerization, and the reductive elimination from **3** have been taken from experimental values reported in our previous works with the same system.[10,15]

Model I proposes the transmetalation of **1** with $ZnMe_2$ to afford **2** through a ligand-dependent pathway, thus including the formation of intermediates in which the ligand cis to the chlorine has been displaced by $ZnMe_2$.[27] On the other hand, a competitive ligand-independent transmetalation produces **3**, in concordance with the experimental behavior of the system.[28] This model fits well the observed kinetic reaction order relative to the concentration of PPh_3, but not the formation of ZnRfMe (red solid spots in Figure 4A), as it predicts a very low concentration of ZnRfMe until almost all the starting palladium complex has been transformed into **2** and **3**, which is not observed to be the case.

Considering the same set of equations of model I, but adding the formation of ZnRfMe by secondary transmetalation with Rf/Me exchange from complex **1**, through a ligand-dependent pathway sharing the *trans*-[PdClRf($ZnMe_2$)(PPh_3)] intermediate in model I, the overall picture (model II) reproduces very well the formation of ZnRfMe. Thus, the early intuition of van Asselt and Elsevier,[9] about the origin of homobiaryls in the reaction of [PdBzBr(ArBIAN)] (Bz = benzyl; Ar-BIAN = bis(arylimino)acenaphthene) with ZnTolCl, finds full support

DOI: 10.1021/acs.organomet.6b00660
Organometallics 2016, 35, 3604−3611

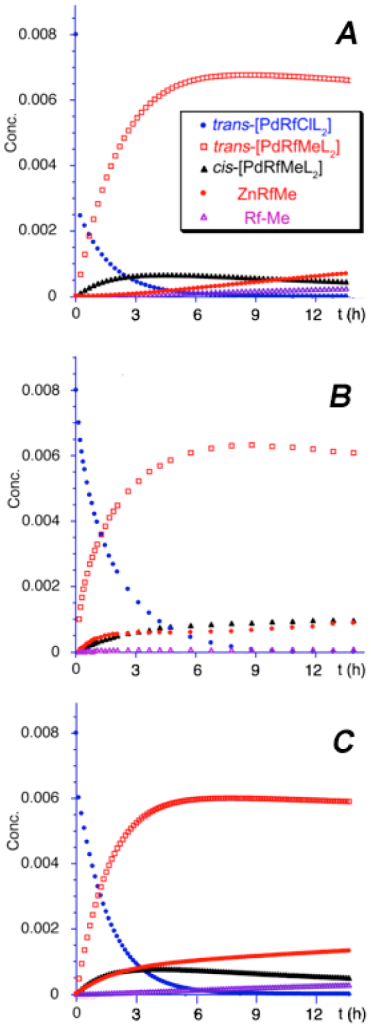

Figure 4. Experimental plot (B) for the transmetalation reaction of $[PdRfCl(L)_2]$ (**1**) with $ZnMe_2$ and kinetic simulations following model I (A) or model II (C). The plots are shown as concentration versus time, using as starting concentrations [**1**] = 8×10^{-3} M, $[ZnMe_2] = 8 \times 10^{-2}$ M, and $[PPh_3] = 4 \times 10^{-3}$ M.

Scheme 5. Overall Mechanism of the Transformations in the Reaction between $[PdRfCl(PPh_3)_2]$ (1) and $ZnMe_2$

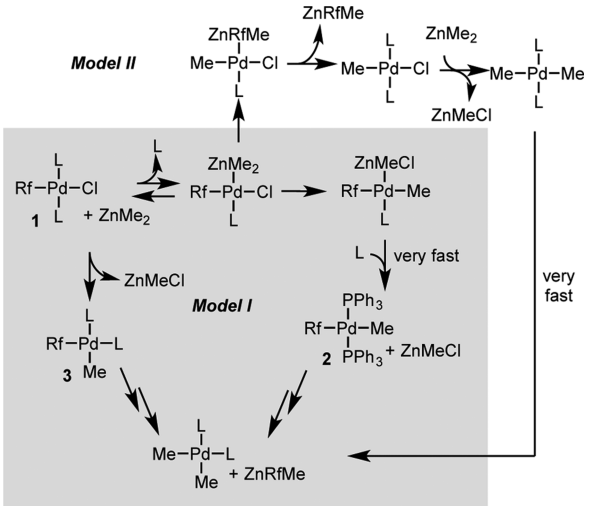

here for the cross-coupling processes of sp^2–sp^3 carbons in which the direct reaction of $ZnMe_2$ and *trans*-$[PdRfCl(PPh_3)_2]$ is confirmed as the dominant transmetalation mechanism when the concentration of *trans*-$[PdRfCl(PPh_3)_2]$ is high.

Model II was used for the least-squares fitting of the set of experimental data of reactions carried out with different concentrations of PPh_3, affording the kinetic rate constants for the transmetalation processes. The reaction profile and the experimental $\Delta G^{\ddagger}$ values from these fittings are shown in Figure 5.

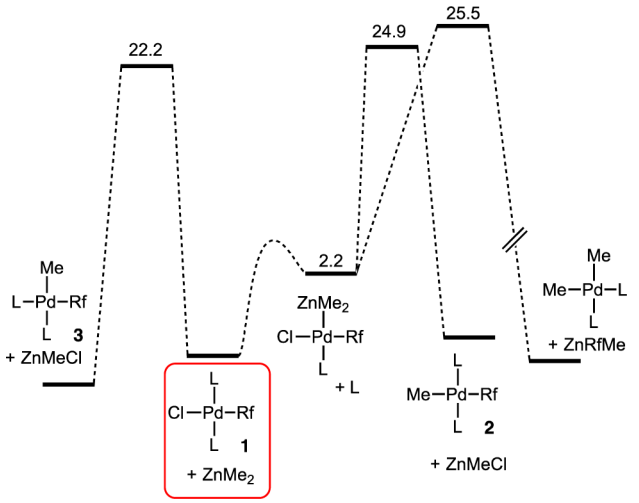

Figure 5. Experimental profile for the transmetalation pathways in the reaction between *trans*-$[PdRfCl(PPh_3)_2]$ (**1**) and $ZnMe_2$. Free energies are given in kcal mol^{-1}.

Obviously Figure 5 cannot reflect the effect of $[PPh_3]$ on the observed rates. At low PPh_3 concentration, the equilibrium leading to formation of the intermediate $[PdRfCl(PPh_3)(ZnMe_2)]$ is shifted to the right, and the transmetalation to form **2** is the fastest process. However, at moderate PPh_3 concentration the transmetalation reactions to form **2** or **3** have almost the same rate.

CONCLUSIONS

This study shows that unwanted Ar/Me transmetalations leading to ZnArMe can take place on *trans*-$[PdArXL_2]$ complexes, and also on *cis* and *trans*-$[PdArMeL_2]$. The exchange is faster on *trans*-$[PdArXL_2]$ than on $[PdArMeL_2]$ complexes, but their activation energies and also the desired transmetalations (Cl/Me exchange) are not very dissimilar; thus, all of the exchanges are accessible at room temperature. Under these circumstances, the specific features of the alkyl, aryl, or halide groups involved, and the ancillary ligands, can be decisive. The faster pathways for the undesired Ar/Me exchange involve ligand-dependent associative substitution of phosphine by $ZnMe_2$ on the square-planar complexes, but direct (ligand-"independent") exchange pathways are also accessible, at least in *trans*-$[PdArMeL_2]$ complexes.

In catalysis, the formation of ZnArR (R = alkyl) derivatives leads to homocoupling products and should be avoided. The addition of excess phosphine reduces not only the formation rate of ZnArR but also the transmetalation reaction rate. On the other hand, if the reductive elimination is slow (as this usually happens when sp^3 carbons are involved), the aryl/alkyl exchange on the coupling intermediates $[PdArRL_2]$ takes

DOI: 10.1021/acs.organomet.6b00660
Organometallics 2016, 35, 3604–3611

place at a non-negligible rate. Thus, the use of ligands bearing some ability to induce faster reductive eliminations is highly desirable.

EXPERIMENTAL SECTION

General Methods. All reactions were carried out under N_2 or Ar in THF dried using a Solvent Purification System (SPS). NMR spectra were recorded on Bruker ARX 300, AV 400, and AV 500 instruments equipped with variable-temperature probes. Chemical shifts are reported in ppm from tetramethylsilane (^{1}H) and CCl_3F (^{19}F), with positive shifts downfield, at ambient probe temperature unless otherwise stated. The temperature for the NMR probe was calibrated with an ethylene glycol standard (high temperature) and with a methanol standard (low temperature).[29] In the ^{19}F and ^{31}P NMR spectra measured in nondeuterated solvents, a coaxial tube containing acetone-d_6 was used to maintain the lock ^{2}H signal, and the chemical shifts are reported from the CCl_3F signal in deuterated acetone. The compounds *trans*-[PdRfMe(PPh_3)$_2$] (**2**) and *cis*-[PdRfMe(PPh_3)$_2$] (**3**) were prepared as reported in the literature.[10]

Kinetic Experiments. In a standard experiment a solution of the palladium complex *trans*-[PdRfCl(PPh_3)$_2$] (**1**), *trans*-[PdRfMe(PPh_3)$_2$] (**2**), or *cis*-[PdRfMe(PPh_3)$_2$] (**3**) (10 mg, 1.13×10^{-2} mmol) and PPh_3 (0−6 mg; $(0-2.3) \times 10^{-2}$ mmol) in THF (0.40 mL) was prepared in a NMR tube and cooled to −96 °C. A 2 M solution of $ZnMe_2$ in toluene (0.20 mL, 0.40 mmol) was added in addition to cold THF to give a final volume of 0.60 mL. Then a coaxial capillary containing acetone-d_6 was added, and the sample was placed into the NMR probe thermostated at 25 °C. The kinetic experiments were followed by ^{31}P NMR or ^{19}F NMR, and concentration−time data were acquired by integration of the NMR signals.

The kinetic models were fit to the measured concentration vs time by nonlinear least-squares (NLLS) regression using the program COPASI.[30] The experimental data were arranged into the matrix, where the columns collect the time-dependent concentration profile of a particular species detected by ^{19}F NMR. The proposed kinetic model was entered into the software program, as well as the known values for the constants measured independently, as specified below. The program produces a list of parameters (rate constants) and constructs a system of simultaneous ordinary differential equations that describe the change in concentration of each species with time. The rate constants were refined by NLLS regression until a best fit was found. The uncertainties of the fitted constants correspond to the standard deviation of the least-squares fitting, given by COPASI. To calculate the kinetic constants from the obtained concentration versus time data, the initial rate method was used. Only the first points (10% of the data) were taken into account to avoid the formation of Pd^0 species that alter the reaction rate.

ASSOCIATED CONTENT

Supporting Information

The Supporting Information is available free of charge on the ACS Publications website at DOI: 10.1021/acs.organomet.6b00660.

Experimental and kinetic details and computational information (PDF)

Cartesian coordinates of calculated structures (XYZ)

AUTHOR INFORMATION

Corresponding Authors

*E-mail for R.Á.: rar@uvigo.es.

*E-mail for J.A.C.: casares@qi.uva.es.

*E-mail for P.E.: espinet@qi.uva.es.

Notes

The authors declare no competing financial interest.

ACKNOWLEDGMENTS

Financial support from the Junta de Castilla y León (Projects GR169 and VA256U13) and the Spanish MINECO (CTQ2013-48406-P, CTQ2012-37734, and CTQ2015-68794-P) is gratefully acknowledged. We also thank the Centro de Supercomputación de Galicia (CESGA, ICTS240-2013 and ICTS257-2014) for generous allocation of computing resources. J.d.P. thanks the Ministerio de Educación, Cultur y Deporte for an FPU grant.

REFERENCES

(1) (a) Negishi, E. *Angew. Chem., Int. Ed.* **2011**, *50*, 6738−6764 (Nobel lecture). (b) *Handbook of Organopalladium Chemistry for Organic Synthesis*; Negishi, E., Ed.; Wiley-Interscience: New York, 2002; Vol. *1*, Part III. (c) Negishi, E.; Zeng, X.; Tan, Z.; Qian, M.; Hu, Q.; Huang, Z. In *Metal-Catalyzed Cross-Coupling Reactions*; de Meijere, A., Diederich, F., Eds.; Wiley-VCH: Weinheim, Germany, 2004; Chapter 15.

(2) For recent reviews of Negishi reaction see: (a) Jana, R.; Pathak, T. P.; Sigman, M. S. *Chem. Rev.* **2011**, *111*, 1417−1492. (b) Wu, X.-F.; Anbarasan, P.; Neumann, H.; Beller, M. *Angew. Chem., Int. Ed.* **2010**, *49*, 9047−9050. Valente, C.; Belowich, M. E.; Hadei, N.; Organ, M. G. *Eur. J. Org. Chem.* **2010**, *23*, 4343−4354. (c) Phapale, V. B.; Cardenas, D. *Chem. Soc. Rev.* **2009**, *38*, 1598−1607. (d) Wuertz, S.; Glorius, F. *Acc. Chem. Res.* **2008**, *41*, 1523−1533. (e) Fu, G. C. *Acc. Chem. Res.* **2008**, *41*, 1555−1564. (f) Jin, L.; Lei, A. *Org. Biomol. Chem.* **2012**, *10*, 6817. (g) Valente, C.; Çalimsiz, S.; Hoi, K. H.; Mallik, D.; Sayah, M.; Organ, M. G. *Angew. Chem., Int. Ed.* **2012**, *51*, 3314−3332.

(3) Recent examples of the Negishi reaction involving the cross-coupling of sp^3 carbon atoms: (a) Berretta, G.; Coxon, G. D. *Tetrahedron Lett.* **2012**, *53*, 214−216. (b) Duez, S.; Steib, A. K.; Knochel, P. *Org. Lett.* **2012**, *14*, 1951−1953. (c) Duplais, C.; Krasovskiy, A.; Lipshutz, B. H. *Organometallics* **2011**, *30*, 6090−6097. (d) Tanaka, M.; Hikawa, H.; Yokoyama, Y. *Tetrahedron* **2011**, *67*, 5897−5901. (e) Hunter, H. N.; Hadei, N.; Blagojevic, V.; Patschinski, P.; Achonduh, G. T.; Avola, S.; Bohme, D. K.; Organ, M. G. *Chem. - Eur. J.* **2011**, *17*, 7845−7851. (f) Krasovskiy, A.; Thomé, I.; Graff, J.; Krasovskaya, V.; Konopelski, P.; Duplais, C.; Lipshutz, B. H. *Tetrahedron Lett.* **2011**, *52*, 2203−2205. (g) Zhang, T.; Gao, X.; Wood, H. B. *Tetrahedron Lett.* **2011**, *52*, 311−313. (h) Hadei, N.; Achonduh, G. T.; Valente, C.; O'Brien, C. J.; Organ, M. G. *Angew. Chem., Int. Ed.* **2011**, *50*, 3896−3899. (i) Nishihara, Y.; Okada, Y.; Jiao, J.; Suetsugu, M.; Lan, M.-T.; Kinoshita, M.; Iwasaki, M.; Takagi, K. *Angew. Chem., Int. Ed.* **2011**, *50*, 8660−8664. (j) Calimsiz, S.; Organ, M. G. *Chem. Commun.* **2011**, *47*, 5181. (k) Bernhardt, S.; Manolikakes, G.; Kunz, T.; Knochel, P. *Angew. Chem., Int. Ed.* **2011**, *50*, 9205−9209.

(4) Reviews covering the cross-coupling of sp^3 carbons: (a) Li, H.; Seechurn, C. C. C. J.; Colacot, T. *ACS Catal.* **2012**, *2*, 1147−1164. (b) Netherton, M. R.; Fu, G. C. *Adv. Synth. Catal.* **2004**, *346*, 1525−1532. (c) Frisch, A. C.; Beller, M. *Angew. Chem., Int. Ed.* **2005**, *44*, 674−688.

(5) (a) McCann, L. C.; Hunter, H. N.; Clyburne, J. A. C.; Organ, M. G. *Angew. Chem., Int. Ed.* **2012**, *51*, 7024−7027. (b) McCann, L. C.; Organ, M. G. *Angew. Chem., Int. Ed.* **2014**, *53*, 4386−4389 and references therein.

(6) (a) García-Melchor, M.; Fuentes, B.; Casares, J. A.; Ujaque, G.; Lledós, A.; Maseras, F.; Espinet, P. *J. Am. Chem. Soc.* **2011**, *133*, 13519−13526. (b) Fuentes, B.; Garcia-Melchor, M.; Lledós, A.; Maseras, F.; Casares, J. A.; Ujaque, G.; Espinet, P. *Chem. - Eur. J.* **2010**, *16*, 8596−8599.

(7) (a) Thaler, T.; Haag, B.; Gavryushin, A.; Schober, K.; Hartmann, E.; Gschwind, R. M.; Zipse, H.; Mayer, P.; Knochel, P. *Nat. Chem.* **2010**, *2*, 125−130. (b) Haas, D.; Hammann, J. M.; Greiner, R.; Knochel, P. *ACS Catal.* **2016**, *6*, 1540−1552.

(8) See for instance: Gioria, E.; Martínez-Ilarduya, J. M.; Espinet, P. *Organometallics* **2014**, *33*, 4394−4400.

DOI: 10.1021/acs.organomet.6b00660
Organometallics 2016, 35, 3604−3611

(9) van Asselt, R.; Elsevier, C. J. *Organometallics* **1994**, *13*, 1972−1980.
(10) Casares, J. A.; Espinet, P.; Fuentes, B.; Salas, G. *J. Am. Chem. Soc.* **2007**, *129*, 3508−3509.
(11) For recent studies on the transmetalation of aryl- and allylzinc see: (a) Liu, Q.; Lan, Y.; Liu, J.; Li, G.; Wu, Y. D.; Lei, A. *J. Am. Chem. Soc.* **2009**, *131*, 10201−10210. (b) Li, J.; Jin, L.; Liu, C.; Lei, A. *Chem. Commun.* **2013**, *49*, 9615−9617. (c) Li, J.; Jin, L.; Liu, C.; Lei, A. *Org. Chem. Front.* **2014**, *1*, 50−53. (d) Yang, Y.; Mustard, T. J. L.; Cheong, P. H.-Y.; Buchwald, S. L. *Angew. Chem., Int. Ed.* **2013**, *52*, 14098−14102.
(12) These are reactions in which an organopalladium complex acts as an arylating or alkylating reagent toward another metal halide, such ZnRX. The reaction has been also reported and studied for the Stille cross-coupling: Pérez-Temprano, M. H.; Nova, A.; Casares, J. A.; Espinet, P. *J. Am. Chem. Soc.* **2008**, *130*, 10518−10519.
(13) Pérez-Rodríguez, M.; Braga, A.A. C.; García-Melchor, M.; Pérez-Temprano, M. H.; Casares, J. A.; Ujaque, G.; de Lera, A. R.; Álvarez, R.; Maseras, F.; Espinet, P. *J. Am. Chem. Soc.* **2009**, *131*, 3650−3657 and references therein.
(14) Note, for instance, that Ar−Ar coupling of perhalogenated aryls has such a high activation energy that it allows for the existence of many very stable *cis*-[$PdAr_2L_2$] complexes: (a) Usón, R.; Fornies, J. *Adv. Organomet. Chem.* **1988**, *28*, 219−297. (b) Alonso, M. A.; Casares, J. A.; Espinet, P.; Martinez-Ilarduya, J. M.; Perez-Briso, C. *Eur. J. Inorg. Chem.* **1998**, *1998*, 1745−1753. (c) Espinet, P.; Martínez-Ilarduya, J. M.; Perez-Briso, C.; Casado, A. L.; Alonso, M. A. *J. Organomet. Chem.* **1998**, *551* (1−2), 9−20. (d) Bartolomé, C.; Espinet, P.; Villafañe, F.; Giesa, S.; Martin, A.; Orpen, A. G. *Organometallics* **1996**, *15*, 2019−2028.
(15) delPozo, J.; Gioria, E.; Casares, J. A.; Álvarez, R.; Espinet, P. *Organometallics* **2015**, *34*, 3120−3128.
(16) The details of both approaches (kinetic evolutions and mathematical workup for the experimental studies; structural data for the calculations) are too long and are given as Supporting Information.
(17) Except with alternative approaches: for instance, when the reverse reaction can be studied. See an example in ref 12.
(18) The oxidative addition of RfI to $Pd(PPh_3)_4$ produces initially *cis*-[$PdRfI(PPh_3)_2$], which then isomerizes to the trans isomer. See: Casado, A. L.; Espinet, P. *Organometallics* **1998**, *17*, 954−959.
(19) For brevity we do not specify at this time the Pd isomer involved; thus, we use a general representation for cis and trans. Note, however, that isomerization can occur during transmetalation. Note also that these transmetalations are highly reversible, regardless of the displacement of the equilibrium to one side or the other.
(20) Note, however, that the amount of **3** formed during the reaction is so small that this result does not affect the overall behavior of the disappearance of **1**.
(21) The rate of the reactions (whether with or without added PPh_3) is also very sensitive to the presence of Pd^0 (presumably $Pd(PPh_3)_2$), which is eager to coordinate more PPh_3 to produce [$Pd(PPh_3)_3$]. The consequence is that, since reductive elimination is retarded by free PPh_3, the formation of palladium(0) by reductive elimination has an autocatalytic effect on the reductive elimination. This effect would mislead the interpretation of the reaction rates measured in the absence of added PPh_3.
(22) The kinetic experiments have been developed with $C_6Cl_2F_3$ (Rf) (which provides simple NMR spectra with more reliable integrations) and PPh_3. The DFT study was developed with a simpler model (Ar = C_6F_5 (Pf) and PPh_3 as ligand). We have shown that there is no significant difference in activation energies for C_6F_5 instead of $C_6Cl_2F_3$.
(23) Frisch, M. J.; Trucks, G. W.; Schlegel, H. B.; Scuseria, G. E.; Robb, M. A.; Cheeseman, J. R.; Scalmani, G.; Barone, V.; Mennucci, B.; Petersson, G. A.; Nakatsuji, H.; Caricato, M.; Li, X.; Hratchian, H. P.; Izmaylov, A. F.; Bloino, J.; Zheng, G.; Sonnenberg, J. L.; Hada, M.; Ehara, M.; Toyota, K.; Fukuda, R.; Hasegawa, J.; Ishida, M.; Nakajima, T.; Honda, Y.; Kitao, O.; Nakai, H.; Vreven, T.; Montgomery, J. A.; Peralta, J. E.; Ogliaro, F.; Bearpark, M.; Heyd, J. J.; Brothers, E.; Kudin, K. N.; Staroverov, V. N.; Kobayashi, R.; Normand, J.; Raghavachari, K.; Rendell, A.; Burant, J. C.; Iyengar, S. S.; Tomasi, J.; Cossi, M.; Rega, N.; Millam, J. M.; Klene, M.; Knox, J. E.; Cross, J. B.; Bakken, V.; Adamo, C.; Jaramillo, J.; Gomperts, R.; Stratmann, R. E.; Yazyev, O.; Austin, A. J.; Cammi, R.; Pomelli, C.; Ochterski, J. W.; Martin, R. L.; Morokuma, K.; Zakrzewski, V. G.; Voth, G. A.; Salvador, P.; Dannenberg, J. J.; Dapprich, S.; Daniels, A. D.; Farkas; Foresman, J. B.; Ortiz, J. V.; Cioslowski, J.; Fox, D. J. *Gaussian 09, Revision B.01*; Gaussian, Inc., Wallingford, CT, 2009.
(24) See the Supporting Information for data regarding PMe_3.
(25) A maximum rate limit without ligand substitution was estimated, assuming that this was the only pathway under the maximum concentration of PPh_3 used. Conversely, assuming this maximum value, a minimum value for the rate of the pathway involving the ligand substitution was obtained (see the Supporting Information).
(26) The palladium and zinc interaction does not have kinetic relevance. We have previously characterized computationally these kinds of bimetallic complexes: (a) Álvarez, R.; de Lera, A. R.; Aurrecoechea, J. M.; Durana, A. *Organometallics* **2007**, *26*, 2799−2802. (b) González-Pérez, A. B.; Álvarez, R.; Faza, O. N.; de Lera, A. R.; Aurrecoechea, J. M. *Organometallics* **2012**, *31*, 2053−2058. (c) Lorenzo, P.; Aurrecoechea, J. M.; de Lera, A. R.; Álvarez, R. *Eur. J. Org. Chem.* **2013**, *2013*, 2621−2626. (d) Arrate, M.; Durana, A.; Lorenzo, P.; de Lera, A. R.; Álvarez, R.; Aurrecoechea, J. M. *Chem. - Eur. J.* **2013**, *19*, 13893−13900.
(27) The kinetic scheme does not presume any interaction between Zn and chlorine or any other atom in the intermediate formed by substitution of PPh_3 by $ZnMe_2$.
(28) For the stronger σ-donor ligand $PMePh_2$ the direct (ligand-independent) substitution pathway seems to be dominant[6]
(29) Ammann, C.; Meier, P.; Merbach, A. E. *J. Magn. Reson.* **1982**, *46*, 319−321.
(30) Complex pathway simulator: Hoops, S.; Sahle, S.; Gauges, R.; Lee, C.; Pahle, J.; Simus, N.; Singhal, M.; Xu, L.; Mendes, P.; Kummer, U. *Bioinformatics* **2006**, *22*, 3067−3074.

DOI: 10.1021/acs.organomet.6b00660
Organometallics 2016, 35, 3604−3611